SEMARAK ILMU PUBLISHING

Journal of Advanced Research in Applied Sciences and Engineering Technology

Journal homepage:
https://semarakilmu.com.my/journals/index.php/applied_sciences_eng_tech/index
ISSN: 2462-1943

Tailoring Precursor Concentration for Low-Temperature Synthesis of ZnO Nanostructures for Piezoelectric Nanogenerator Applications

Nurfatini Atiqrah Khairul Azhar[1,2], Mohd Firdaus Malek[1,2*], Maryam Mohammad[1,2,3], Kevin Alvin Eswar[1,4], Nur Fairuz Rostan[1,2], Zahidah Othman[1,2], Mohamad Dzulfiqar Bakri[1,2], Muhamad Kamil Yaakob[1,2], Asiah Mohd Nor[1,2], Ruziana Mohamed[1,2], Rosdiyana Hisam[2] and Tetsuo Soga[5]

[1] NANO-SciTech Lab (NST), Centre for Functional Materials and Nanotechnology (CFMN), Institute of Science (IOS), Universiti Teknologi MARA (UiTM), 40450 Shah Alam, Selangor, Malaysia
[2] Faculty of Applied Sciences, Universiti Teknologi MARA (UiTM), 40450 Shah Alam, Selangor, Malaysia
[3] Department of Physics, Faculty of Applied Sciences, Universiti Teknologi MARA (UiTM), Perak Branch, Tapah Campus, Tapah Road, 35400 Perak, Malaysia
[4] Department of Physics, Faculty of Applied Sciences, Universiti Teknologi MARA (UiTM), Sabah Branch, Tawau Campus, 91000 Sabah, Malaysia
[5] Department of Electrical and Mechanical Engineering, Nagoya Institute of Technology (NITech), Showa-ku, Gokiso-cho, Nagoya, 466-8555, Japan

ARTICLE INFO

Article history:
Received 10 February 2026
Received in revised form 30 May 2026
Accepted 2 June 2026
Available online 14 August 2026

ABSTRACT

As the global demand for sustainable energy solutions intensifies, piezoelectric nanogenerators (PENG) have emerged as promising candidates for powering wearable and portable devices, aligning with the United Nations' 2030 Agenda for Sustainable Development Goals, particularly Goal 7 (Affordable and Clean Energy). Zinc oxide (ZnO) nanostructures, known for their exceptional piezoelectric and semiconducting properties, are also biocompatible and environmentally friendly, making them pivotal in advancing PENG technology. Although extensively studied, ZnO nanostructures still face challenges in achieving high crystallinity and controlled morphology at low temperatures, particularly for flexible substrates. Conventional methods like chemical vapor deposition (CVD) and hydrothermal synthesis require high temperatures and long durations, limiting their compatibility with temperature-sensitive materials such as polyethylene terephthalate (PET). In this study, ZnO nanostructures were synthesised using a microwave-assisted sonochemical technique, focusing on the effect of varying precursor concentrations (0.01M, 0.0125M, 0.025M, 0.05M, 0.075M, and 0.1M) on structural and electrical characteristics. X-ray diffraction (XRD) and field emission scanning electron microscopy (FESEM) analyses were conducted to explain the crystal structure and surface morphology of the synthesised ZnO, while oscilloscope measurements were used to evaluate voltage output for piezoelectric performance. XRD analysis confirmed the structures of ZnO across all precursor concentrations, with variations in peak intensity and crystallite size indicating the influence of concentration on crystallinity and preferred orientation. FESEM images revealed distinct morphological changes with increasing precursor concentration. Oscilloscope results highlighted the correlation between optimised ZnO nanostructure morphology and enhanced voltage output, confirming the significance of precursor concentration in achieving efficient energy harvesting. The microwave-assisted sonochemical technique, characterised by its rapid reaction time and low-temperature synthesis (100°C), proved to be an effective method for growing ZnO nanostructures for PENG. This method's

* *Corresponding author.*
E-mail address: mfmalek07@uitm.edu.my; mfmalek07@gmail.com

Keywords:
ZnO; Concentration; Microwave; Nanostructures; Nanogenerator

ability to produce highly crystalline ZnO at low temperature is particularly advantageous for flexible substrates in wearable electronics and energy harvesting applications. The findings underscore the critical role of precursor concentration in tailoring ZnO structural and electrical properties, offering valuable insights into optimising ZnO nanostructures for PENG applications. This work contributes to the development of sustainable and efficient energy harvesting technologies, demonstrating the potential of ZnO nanostructures in next-generation wearable and portable devices.

1. Introduction

The global shift towards sustainable energy solutions is accelerating research into alternative energy-harvesting technologies, driven by the urgent need to reduce reliance on conventional energy sources and mitigate the environmental impact of fossil fuels [1-3]. Among the various technologies under investigation, piezoelectric nanogenerators (PENG) have emerged as a highly promising solution for powering wearable and portable electronic [4-7]. These devices, which convert mechanical energy into electrical energy using piezoelectric materials, offer an eco-friendly and scalable approach to energy harvesting [8]. The ability of PENG to power small electronics by harvesting biomechanical energy opens exciting possibilities in fields ranging from healthcare monitoring to next-generation consumer electronics, aligning with the United Nations' Sustainable Development Goal (SDG 7) of ensuring access to affordable and clean energy [9].

Zinc oxide (ZnO), a wide-bandgap semiconductor with intrinsic piezoelectricity, has attracted considerable attention as a core material for PENG applications due to its outstanding combination of piezoelectric, and semiconducting properties [10-12]. Beyond its remarkable electrical performance, ZnO is biocompatible, abundant, and environmentally friendly, further establishing its potential as a material for sustainable energy solutions [13, 14]. One of ZnO's most attractive features is its versatility in forming diverse nanostructures such as nanorods, nanowires, and nanosheets, each of which can be tailored to specific applications by adjusting synthesis conditions [15-17]. Despite extensive research on ZnO nanostructures, key challenges remain in achieving high crystallinity and controlled morphology at low temperatures, especially for flexible substrates used in wearable electronics. Most conventional synthesis techniques, such as chemical vapor deposition (CVD) and hydrothermal methods, are limited by high processing temperatures and prolonged reaction times, making them less suitable for integrating with temperature-sensitive materials like polyethylene terephthalate (PET) [18].

Recent advancements in low-temperature synthesis techniques have opened new doors for producing high-quality ZnO nanostructures while preserving substrate integrity. Among these, the microwave-assisted sonochemical method stands out for its rapid reaction kinetics, uniform heating, and ability to synthesize nanomaterials at temperatures as low as 100°C [19, 20]. This technique leverages the synergistic effects of microwave irradiation and ultrasonic cavitation to promote homogeneous nucleation and controlled growth of nanostructures, resulting in highly crystalline materials with tunable properties [21, 22]. However, while the potential of this method for ZnO synthesis is well recognized, the systematic exploration of precursor concentration as a critical parameter in determining the structural and piezoelectric performance of ZnO nanostructures remains largely unexplored.

Precursor concentration plays a pivotal role in governing the nucleation and growth dynamics during ZnO synthesis. Variations in concentration can significantly influence the morphology, crystallinity, and defect density of the resulting nanostructures, which in turn affect their electrical and mechanical properties [23, 24]. Although several studies have investigated the effect of

precursor concentration on ZnO morphology, most have focused on high-temperature synthesis methods or provided limited insights into how these variations impact piezoelectric performance at low temperatures [25]. This represents a crucial gap in the current body of knowledge, particularly for researchers seeking to optimize ZnO nanostructures for practical applications in wearable and portable energy-harvesting devices

In this study, we address this gap by synthesizing ZnO nanostructures using a microwave-assisted sonochemical technique at a fixed low temperature of 100°C, systematically varying precursor concentrations to investigate their effect on structural, morphological, and piezoelectric properties [26]. The use of a low-temperature synthesis method is particularly advantageous for flexible substrates, making this study highly relevant for the growing field of wearable electronics [27]. Comprehensive characterization of the synthesized ZnO nanostructures is performed using X-ray diffraction (XRD) and field emission scanning electron microscopy (FESEM) to evaluate crystallinity and surface morphology, while oscilloscope measurements are employed to assess their piezoelectric voltage output. By correlating the structural characteristics with electrical performance, this work provides new insights into the relationship between precursor concentration and piezoelectric efficiency.

What sets this research apart is its focus on optimizing ZnO synthesis at low temperatures, offering a novel perspective on controlling nanostructure properties through a single, critical parameter that is precursor concentration. Unlike previous studies that emphasize high-temperature methods or doping strategies, this work demonstrates how precursor concentration alone can be strategically manipulated to enhance the crystallinity and piezoelectric output of ZnO [28-32]. The findings not only highlight the importance of precursor concentration in tailoring ZnO properties but also establish a scalable and substrate-friendly approach for fabricating high-performance nanostructures for energy harvesting.

Ultimately, this study contributes to the advancement of sustainable energy technologies by providing a deeper understanding of how low-temperature synthesis conditions affect the structural and functional properties of ZnO nanostructures. The results presented here offer valuable guidance for future research aimed at developing efficient, flexible, and environmentally friendly energy-harvesting devices for wearable and portable applications.

2. Methodology

2.1 Materials

Zinc Acetate Dihydrate [$Zn(CH_3CO_2)_2{\cdot}2H_2O$], Monoethanolamine [MEA (C_2H_7NO)], Ethanol (CH_3CH_2OH), Zinc Nitrate Hexahydrate [$Zn(NO_3)_2.6H_2O$], Hexamethylenetetramine [HMTA ($C_6H_{12}N_4$)] and Deionised Water (DI Water).

2.2 Preparation of ZnO seeded layer deposited on PET substrate

The preparation of ZnO seed layer first starts with the cleaning of flexible polyethylene terephthalate (PET) of a size of 2.5cm x 3.5cm as the substrate. The PET were cleaned with ethanol and DI water for 10 minutes each in an ultrasonic bath and then were left to dry in the air to remove the moisture. Ultrasonic-assisted dip-coating technique was used to coat the PET on both sides. The seed solution was prepared beforehand by dissolving zinc acetate dehydrate [$Zn(CH_3CO_2)_2{\cdot}2H_2O$] in ethanol to obtain the concentration of 0.4 mol/L. Monoethanolamine, [MEA (C2H7NO)] which acts as stabilizer was then added and the MEA:zinc acetate molar ratio was kept constant at 1:1. The solution was stirred to obtain a uniform and clear solution. Next, after attaching the substrate to the dip-coater, the substrates were dipped into the solution for 10 seconds with both upward and

downward speed of 40 mm/s to obtain a uniform distributed seed layer across the PET. This process was repeated five times with an interval of a heating process of 100°C for 10 minutes after each dip. The heating process was done to eliminate the solvent residue and ensure strong adhesion of the seed layer. Finally, the ZnO seed layer was heated to 100°C for 25 minutes to improve the crystalline quality.

2.3 Growth of ZnO nanostructures using microwave-assisted sonochemical technique

Next, an aqueous solution of zinc nitrate hexahydrate [$Zn(NO_3)_2.6H_2O$] and hexamethylenetetramine [HMTA, $C_6H_{12}N_4$] with different precursor concentration (0.01M, 0.0125M, 0.025M, 0.05M, 0.075M, and 0.1M) were mixed with 1000ml of DI water. The solution was stirred for 30 minutes to achieve homogeneous solution. Subsequently, the solution underwent ultrasonic treatment within a water bath at a temperature of 50°C for a duration of 30 minutes, employing a 40 kHz frequency (Hwasin Technology Powersonic 405). The solution later was allowed to age for 1 hour at room temperature. After that, the solution was given another 1 hour of stirring without adding any heat. Later, the solution was transferred into a 100ml Schott bottle and the PET substrate was submerged into the prepared solution. The microwave was set to 200-watt power for a fix of 30 minutes deposition time. Lastly, the substrate was removed from the solution, washed with DI water to remove the residues on the surface and left to dry in air.

2.4 Fabrication of ZnO nanostructures for PENG applications

Lastly, the fabrication process of PENG was conducted. A layer of battery-grade Aluminium foil will be placed on top of the PET substrate. The Aluminium foil acted as the top electrode while the PET acted as the bottom electrode to ensure the flow of electricity throughout the ZnO PENG. Kapton tape was used to bind them to sustain both material and prevent from inconsistent output results.

2.5 Characterisation methods

The structural properties of ZnO nanostructures were analysed by using X-ray diffraction (XRD, PANalytical X'Pert3 PRO) at 45 kV and 40 mA with Cu-Ka radiation at ca. 2θ = 5º-90º. The surface morphology of the structure of all samples was characterised by field emission scanning electron microscopy (FESEM, Analytical High Resolution Field Emission Scanning Electron Microscope Apreo 2S (Thermo Fischer Scientific). The electrical properties were characterised by using oscilloscope (Keithley 2420 Sourcemeter).

3. Results

3.1 Morphological and structural analysis of ZnO nanostructures

Figure 1 shows the morphological evolution of ZnO nanostructures synthesised at various precursor concentrations (0.01M, 0.0125M, 0.025M, 0.05M, 0.075M and 0.1M) was analysed using FESEM at magnifications of 30,000× and 100,000×. The results reveal that the precursor concentration plays a crucial role in controlling the growth, density, and uniformity of the resulting nanostructures.

At the lowest precursor concentration of 0.01 M, the ZnO structures appear sparse and poorly defined, with isolated nanoparticles scattered across the surface. This morphology is a result of insufficient nucleation caused by the limited availability of Zn^{2+} and OH^- ions. The poor surface

coverage at this concentration would likely hinder the efficiency of the piezoelectric nanogenerator, as the scattered structures provide minimal contact area for mechanical stress transfer [33, 34]. However, as the precursor concentration increases to 0.0125 M, there is a significant improvement in the morphology. The ZnO nanostructures transform into uniform and well-connected nanosheets that cover the substrate in a dense but highly ordered arrangement. These nanosheets are evenly distributed without excessive agglomeration, ensuring a large surface area and strong structural integrity. This morphology is highly desirable for piezoelectric applications, as the continuous nanosheets provide excellent mechanical coupling and enhanced stress transfer during mechanical deformation, which is essential for improving the output performance of the nanogenerator. When the precursor concentration reaches 0.025 M, the nanosheet structure becomes thicker and more complex, forming larger overlapping sheets across the surface. Although the coverage remains high, the increased complexity and irregularity reduce the uniformity observed at 0.0125 M. The hierarchical structure at this concentration may contribute positively to piezoelectric performance. Further increasing the precursor concentration to 0.05 M results in the formation of dense, hierarchical flower-like structures. These highly interconnected structures exhibit significant agglomeration, which compromises the clarity and definition of individual nanosheets. The agglomeration introduces defects and may limit the flexibility of the resulting piezoelectric device. At higher concentrations of 0.075 M and 0.1 M, the ZnO morphology becomes even more densely packed and heavily agglomerated [35]. The excessive availability of ions at these concentrations promotes uncontrolled nucleation and rapid crystal growth, resulting in thick, non-uniform layers that lack the nanosheet morphology observed at lower concentrations. The structural integrity of these samples is compromised, with poor mechanical adaptability and an increased likelihood of defects that can adversely affect the piezoelectric performance.

The results of the morphological analysis clearly indicate that 0.0125 M provides the most balanced and optimised morphology for ZnO nanostructures. The uniform nanosheet network at this concentration offers several advantages, including high surface area for effective charge generation and collection, uniform stress distribution for enhanced piezoelectric response and minimal defects and agglomeration for improved device stability and flexibility. In contrast, concentrations higher than 0.0125 M result in thicker and more irregular structures, while lower concentrations fail to achieve sufficient coverage and connectivity between the nanostructures.

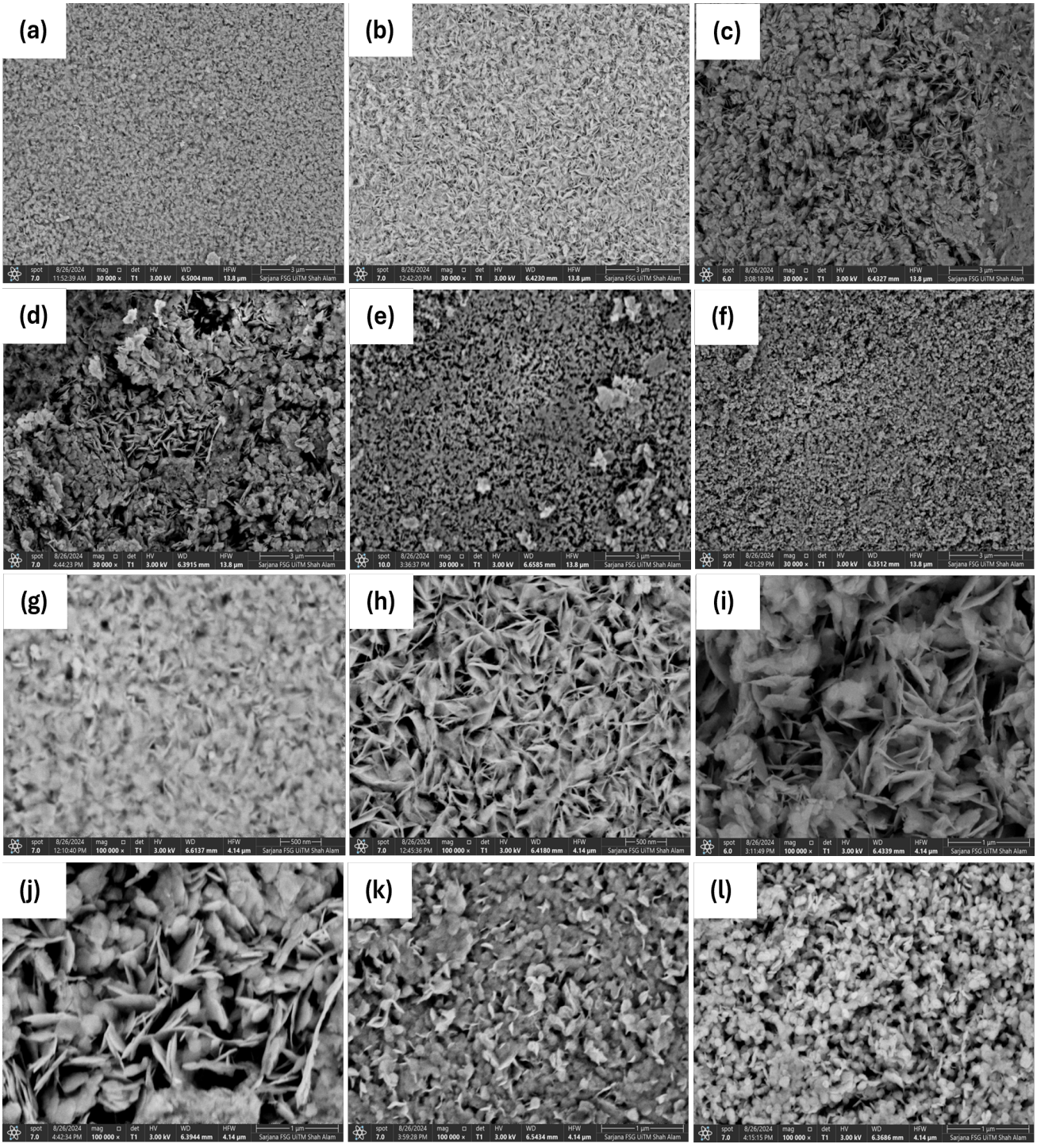

Fig. 1. The surface morphology of the ZnO nanostructures prepared on PET substrate at magnifications 30,000X (a) 0.01M (b) 0.0125M (c) 0.025M (d) 0.05M (e) 0.075M and (f) 0.1M. The surface morphology of the ZnO nanostructures prepared on PET substrate at magnifications 100,000X (g) 0.01M (h) 0.0125M (i) 0.025M (j) 0.05M (k) 0.075M and (l) 0.1M

The structural and morphological characteristics of ZnO films synthesised at varying precursor concentrations were analysed using XRD (JCPDS card no. 03-065-2880). The XRD patterns as shown

in Figure 2, explained that all samples exhibit prominent peaks corresponding to the (200) diffraction plane, confirming the successful synthesis of cubic-phase ZnO. Table 1 summarises the peak position, full-width at half-maximum (FWHM) and crystallite size for all samples. The intensity of the (200) peak vary significantly with different precursor concentrations, indicating differences in crystallinity and crystal growth dynamics. The crystallite size was calculated using the Scherrer equation for the (200) peak and the FWHM was measured for each sample. At low concentrations (0.01M and 0.0125M), the diffraction peaks are relatively sharp and well-defined, indicating high crystallinity and fewer lattice defects. The crystallite size for these samples is larger compared to higher concentrations, with 0.01M and 0.0125M having crystallite sizes of 91.8 nm and 88.5 nm, respectively. These values are consistent with the FESEM images, which show well-aligned and densely packed nanostructures for these concentrations, contributing to enhanced crystal growth along the preferred orientation. As the precursor concentration increases to 0.025M and 0.05M, a slight broadening of the (200) peak is observed, indicating a reduction in crystallite size and increased lattice strain. This broadening corresponds to a slight increase in FWHM compared to the lower concentrations. The crystallite sizes for 0.025M and 0.05M are 83.8 nm and 85.8 nm while the FWHM values remain relatively stable. The FESEM images of these samples reveal a more compact structure with less uniformity, suggesting that higher precursor concentrations result in increased nucleation sites, leading to smaller crystallite sizes and more disordered growth patterns [36]. At the highest concentrations (0.075M and 0.1M), significant broadening of the (200) peak is evident, along with a noticeable reduction in peak intensity. This indicates a substantial decrease in crystallite size and a higher degree of structural disorder. The calculated crystallite sizes for 0.075M and 0.1M are 85.2 nm and 64.1 nm, respectively, with FWHM values of 0.103° and 0.137°. The FESEM images for these samples show densely packed, irregular nanostructures with a rough surface morphology. Such morphology is indicative of rapid nucleation and inhibited crystal growth, which explains the reduced crystallite size and increased defect density at higher precursor concentrations [37, 38].

Table 1
The peak position, FWHM and crystallite size for all samples of varied precursor concentration

Sample	Precursor concentration, Molarity (M)	Peak position, (2θ)	FWHM (degree, °)	Crystallite size (nm)
a)	0.0100M	38.4	0.096	91.8
b)	0.0125M	38.4	0.099	88.5
c)	0.0250M	38.4	0.105	83.8
d)	0.0500M	38.4	0.102	85.8
e)	0.0750M	38.4	0.103	85.2
f)	0.1000M	38.4	0.137	64.1

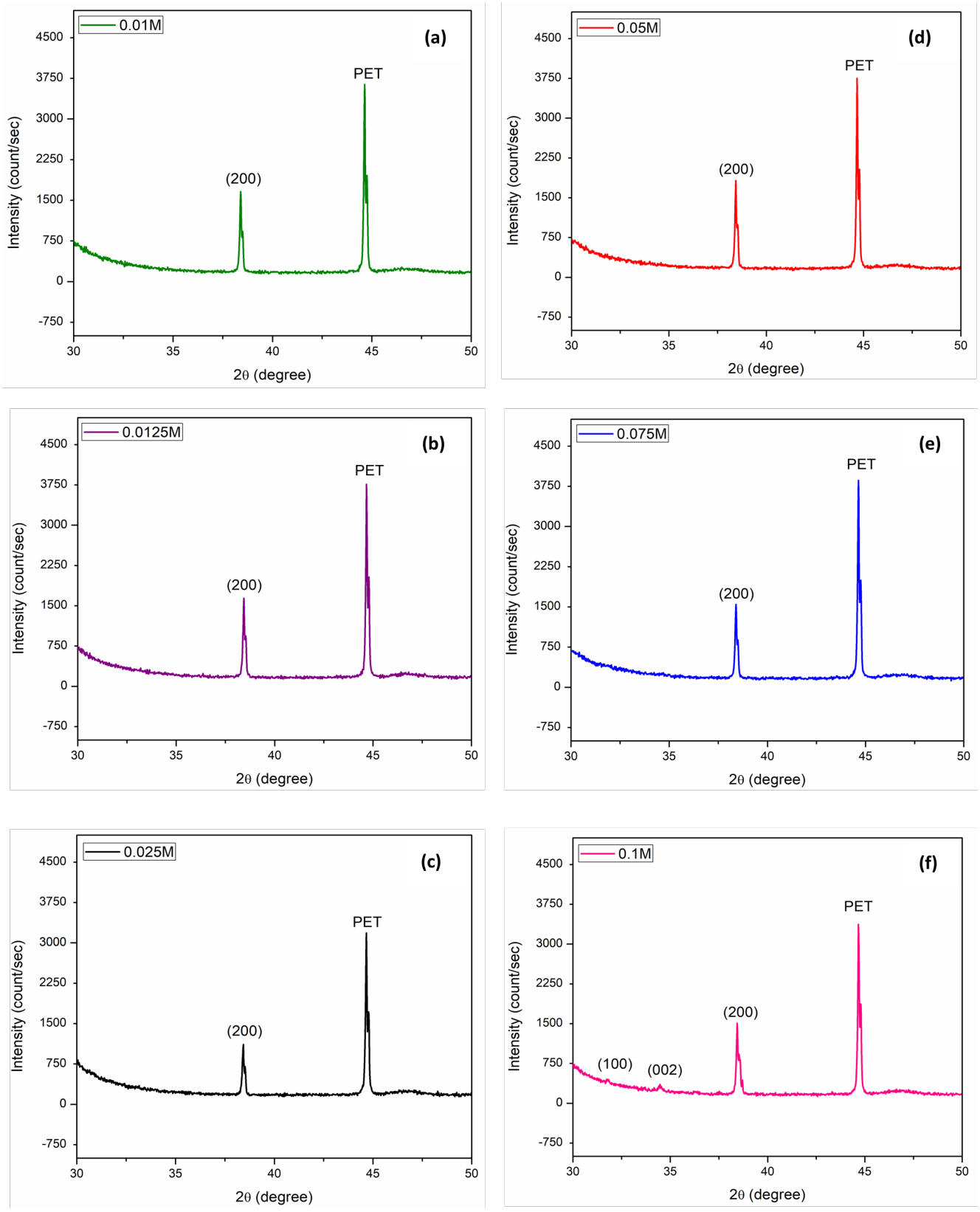

Fig. 2. The XRD analysis of the ZnO nanostructures prepared on PET substrate for PENG application (a) 0.01M, (b) 0.0125M, (c) 0.025M, (d) 0.05M, (e) 0.075M and (f) 0.1M

3.2 Electrical analysis of ZnO nanostructures for PENG applications

The output voltage of ZnO-based piezoelectric nanogenerators was measured for samples prepared using different precursor concentrations, ranging from 0.01M to 0.1M as observed in Figure 3. The electrical performance, specifically the peak-to-peak voltage (V_{pp}), showed a distinct correlation with the morphology of the ZnO nanostructures as observed in the FESEM images. This relationship highlights the importance of optimising precursor concentration to achieve superior piezoelectric performance.

The sample prepared with 0.0125M concentration exhibited the highest output, with a peak-to-peak voltage of approximately 14 V. The corresponding FESEM images revealed a well-defined nanosheet-like morphology that plays a crucial role in enhancing the piezoelectric response. These nanosheets offer several advantages, including a high surface area that increases the effective contact with the substrate, leading to better mechanical stress transfer. The continuous and interconnected structure of the nanosheets helps distribute stress evenly across the surface, improving charge generation [39]. Furthermore, this morphology provides efficient electron transport pathways, minimising energy losses and boosting the overall output voltage [40].

In comparison, the 0.01M sample, while producing a relatively high peak-to-peak voltage of around 8 V, showed less well-defined nanosheet structures. The FESEM image of this sample indicates the presence of thin, sparsely distributed ZnO structures. Although these structures have good alignment, their limited coverage reduces mechanical coupling, which ultimately affects the piezoelectric response. Consequently, the output voltage is lower than that of the 0.0125M sample. As the precursor concentration increased to 0.025M and 0.05M, a transition in morphology was observed. The nanosheets became thicker and more compact, with signs of partial agglomeration. This change in morphology coincided with a reduction in output voltage to approximately 4.5 V. The thicker structures reduce the flexibility of the ZnO film, which impairs stress-transfer efficiency. This decrease in flexibility diminishes the ability of the nanostructures to convert mechanical energy into electrical energy effectively, resulting in lower piezoelectric output. At higher concentrations of 0.075M and 0.1M, the FESEM images showed heavily agglomerated structures, forming a dense, almost bulk-like layer. The corresponding voltage outputs were notably lower, with peak-to-peak voltages of 4 V and 3 V, respectively. The agglomeration at these concentrations results in reduced surface sensitivity and increased rigidity of the ZnO layer. These bulkier structures respond less effectively to mechanical deformation, limiting the generation of piezoelectric charge. Additionally, the agglomeration creates voids and uneven surfaces that contribute to localised stress and charge dissipation, further reducing the output.

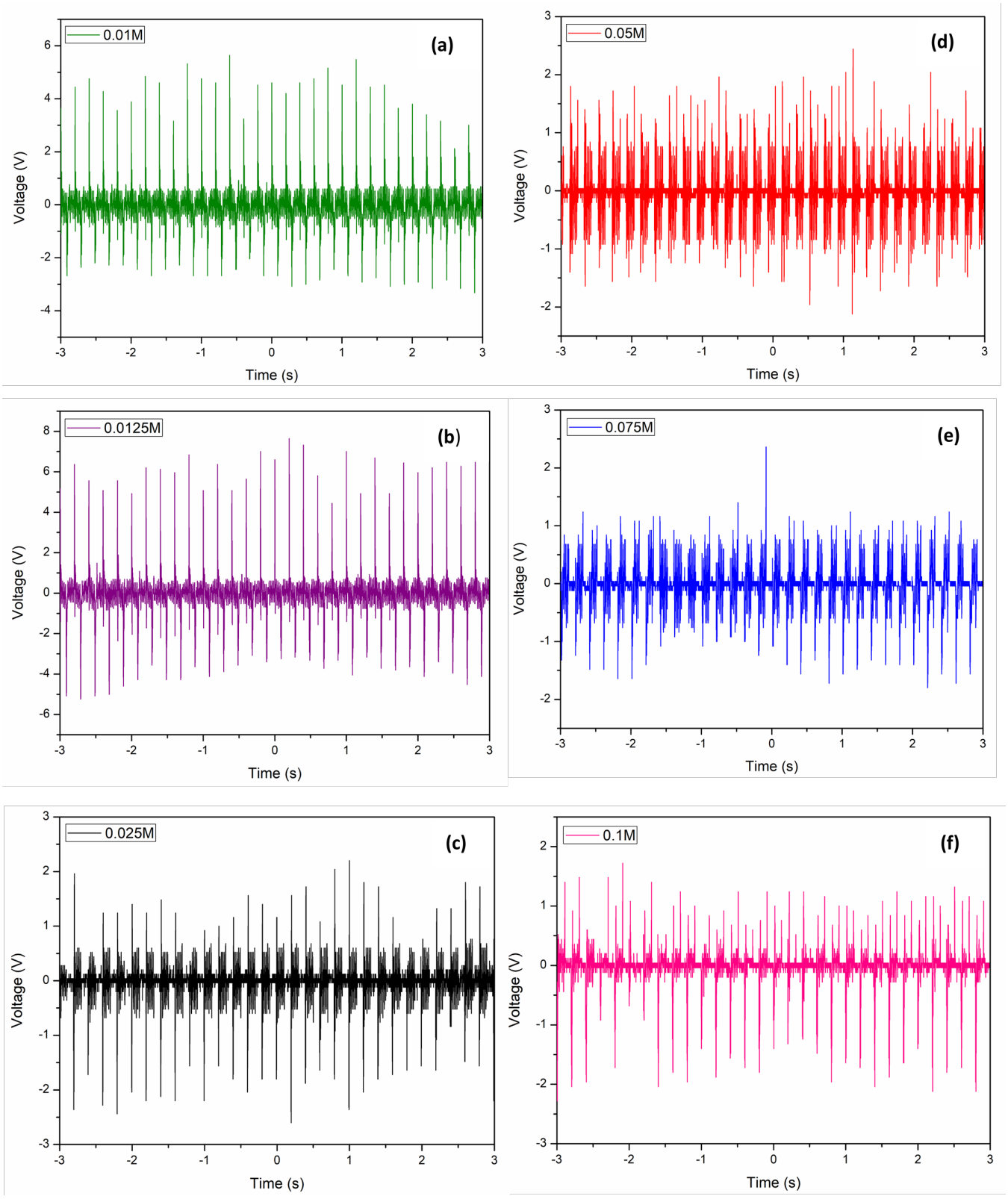

Fig. 3. The output electrical voltage of the PENG measured using oscilloscope (a) 0.01M, (b) 0.0125M, (c) 0.025M, (d) 0.05M, (e) 0.075M and (f) 0.1M

4. Conclusions

This study investigated the synthesis of ZnO nanostructures on PET substrates at varying precursor concentrations, focusing on their structural and piezoelectric properties. Through a combination of XRD, FESEM and electrical measurements, 0.0125 M precursor concentration was determined to be the optimal condition for achieving high-quality ZnO nanostructures with superior piezoelectric performance.

The XRD analysis confirmed the cubic-phase ZnO formation, with the prominent (200) peak observed at all precursor concentrations. The calculated crystallite size and FWHM revealed that 0.0125 M achieved an optimal crystallite size of approximately 88.5 nm with an FWHM of 0.099°. This combination suggests a highly crystalline structure with reduced lattice strain and minimal defect density, critical factors for enhancing the piezoelectric properties. At lower precursor concentrations (0.01 M), the ZnO films exhibited incomplete crystal growth and poor crystallinity, while higher concentrations (≥0.05 M) resulted in excessive nucleation, leading to smaller crystallite sizes and increased lattice disorder, as indicated by the broadening of the diffraction peaks.

FESEM analysis provided crucial insight into the surface morphology evolution across different concentrations. At 0.0125 M, the ZnO nanostructures or specifically nanosheets, displayed a well-defined, dense and uniform morphology. Such a structure is known to facilitate improved charge transfer and reduced recombination losses, thereby enhancing the piezoelectric response [41]. In contrast, films at lower concentrations exhibited sparse and non-uniform growth, which compromises electrical connectivity, while higher concentrations produced agglomerated and irregular structures that introduce defects, thus limiting their performance.

The piezoelectric performance was evaluated through oscilloscope measurements of the generated electrical output under mechanical stimulation. The sample synthesised at 0.0125 M demonstrated a significantly higher peak-to-peak voltage (V_{pp}) of nearly 14 V. This superior performance can be attributed to the synergistic effect of high crystallinity and optimized morphology, which enhances polarization and charge generation in the ZnO nanostructures. The increase in defect density and surface irregularity at higher concentrations is consistent with the reduction in piezoelectric output, reflecting the adverse effect of structural imperfections on charge collection efficiency.

In conclusion, the 0.0125 M precursor concentration offers the most favourable combination of structural integrity, surface morphology, and electrical output, confirming it as the optimal condition for ZnO-based piezoelectric nanogenerators. The findings underline the critical role of precursor concentration in tuning the crystallinity and morphology of ZnO nanostructures, which directly influence the piezoelectric response. These insights provide a strong foundation for the future development of scalable and high-performance piezoelectric devices, with potential applications in self-powered systems and energy harvesting technologies. Future studies should focus on refining other synthesis parameters, such as deposition time and growth temperature, to further improve the performance and consistency of the nanogenerator output.

Acknowledgement
This work was supported by grant no. 600-RMC/GPM CoE 5/3 (106/2022). The authors would like to thank the Research Management Centre (RMC), Universiti Teknologi MARA (UiTM), Malaysia for their support. The authors also thank Mr. Salifairus Mohammad Jafar (UiTM Senior Science Officer), Mr. Mohd Azlan Jaafar (UiTM senior assistant engineer) and Mr. Muhamad Faizal Abd Halim (Assistant Research Officer) for their kind support on this research.

References

[1] Kamaruzaman, D., et al. "Effects of Thermal Annealing on The Morphology and Structural Characteristics of Zinc Oxide Nanopowders for Triboelectric Nanogenerator Applications." Journal of Advanced Research in Fluid Mechanics and Thermal Sciences 99, no. 1 (2022): 17-27. https://doi.org/10.37934/arfmts.99.1.1727.

[2] Sun, J., et al. "A Sustainable and Biodegradable Wood Sponge Piezoelectric Nanogenerator for Sensing and Energy Harvesting Applications." ACS Nano, September 16, 2020. https://doi.org/10.1021/acsnano.0c05493.

[3] Zi, Y., and Z. L. Wang. "Nanogenerators: An Emerging Technology Towards Nanoenergy." APL Materials 5, no. 3 (2017): 074103. https://doi.org/10.1063/1.4977208.

[4] Kamaruzaman, D., et al. "Influence of Heat Treatment on Zinc Oxide Nanostructured Film Grown by Immersion Method for Nanogenerator Application." Materials Today: Proceedings 75 (2023): 31-38. https://doi.org/10.1016/j.matpr.2022.09.584.

[5] Lu, L., W. Ding, J. Liu, and B. Yang. "Flexible PVDF-Based Piezoelectric Nanogenerators." Nano Energy 78 (2020): 105251. https://doi.org/10.1016/j.nanoen.2020.105251.

[6] Yan, J., et al. "Performance Enhancements in Poly(Vinylidene Fluoride)-Based Piezoelectric Nanogenerators for Efficient Energy Harvesting." Nano Energy (2019). https://doi.org/10.1016/j.nanoen.2018.12.010.

[7] Hu, D., M. Yao, Y. Fan, M. Fan, and M. Liu. "Strategies to Achieve High-Performance Piezoelectric Nanogenerators." Nano Energy (2019). https://doi.org/10.1016/j.nanoen.2018.10.053.

[8] Indira, S. S., A. Vaithilingam, K. S. P. Oruganti, F. Mohd, and S. Rahman. "Nanogenerators as a Sustainable Power Source: State of Art, Applications, and Challenges." Nanomaterials 9 (2019): 773. https://doi.org/10.3390/nano9050773.

[9] Jiao, P. "Emerging Artificial Intelligence in Piezoelectric and Triboelectric Nanogenerators." Nano Energy 88 (2021): 106227. https://doi.org/10.1016/j.nanoen.2021.106227.

[10] Tlemcani, S., C. Justeau, K. Nadaud, D. Alquier, and G. Poulin-Vittrant. "Fabrication of Piezoelectric ZnO Nanowires Energy Harvester on Flexible Substrate Coated with Various Seed Layer Structures." Nanomaterials 11 (2021): 1433. https://doi.org/10.3390/nano11061433.

[11] Choi, D., et al. "Transparent, Flexible, and Highly Sensitive Piezocomposite Capable of Harvesting and Monitoring Kinetic Movements of Microbubbles in Liquid." Advanced Functional Materials 33 (2023). https://doi.org/10.1002/adfm.202307607.

[12] Yang, W., Y. Wang, Z. Hou, and C. Li. "A Facile Hot-Pressing Process for Fabricating Flexible Top Electrodes of Piezoelectric ZnO Nanowire Nanogenerators." Nanotechnology 30 (2019). https://doi.org/10.1088/1361-6528/ab3e14.

[13] Ojha, D., et al. "Supersonically Sprayed Flexible ZnO/PVDF Composite Films with Enhanced Piezoelectricity for Energy Harvesting and Storage." International Journal of Energy Research (2023). https://doi.org/10.1155/2023/3074782.

[14] M., M., et al. "Development of Sn-Doped ZnO Based Ecofriendly Piezoelectric Nanogenerator for Energy Harvesting Application." Nanotechnology 31 (2020). https://doi.org/10.1088/1361-6528/ab6b9e.

[15] Kaur, J., and H. Singh. "Fabrication and Analysis of Piezoelectricity in 0D, 1D and 2D Zinc Oxide Nanostructures." Ceramics International 46 (2020): 19401-19407. https://doi.org/10.1016/j.ceramint.2020.04.283.

[16] Yempally, S., P. Magadia, and D. Ponnamma. "Effect of Zn–Fe2O3 Nanomaterials on the Phase Separated Morphologies of Polyvinylidene Fluoride Piezoelectric Nanogenerators." RSC Advances 13 (2023): 33863-33874. https://doi.org/10.1039/d3ra03745b.

[17] Mahmud, A., et al. "A High Performance and Consolidated Piezoelectric Energy Harvester Based on 1D/2D Hybrid Zinc Oxide Nanostructures." Advanced Materials Interfaces 5 (2018). https://doi.org/10.1002/admi.201801167.

[18] Fiaschi, G., et al. "Effect of Laser Annealing on ZnO Nanorods Grown by Chemical Bath Deposition on Flexible Substrate." Applied Surface Science (2018). https://doi.org/10.1016/j.apsusc.2018.07.092.

[19] Ridwan, M., V. Fauzia, and L. Roza. "Synthesis and Characterization of ZnO Nanorods Prepared Using Microwave-Assisted Hydrothermal Method." IOP Conference Series: Materials Science and Engineering 496 (2019). https://doi.org/10.1088/1757-899X/496/1/012018.

[20] Ortega, P., et al. "Multifunctional Environmental Applications of ZnO Nanostructures Synthesized by the Microwave-Assisted Hydrothermal Technique." Applied Surface Science 542 (2021): 148723. https://doi.org/10.1016/j.apsusc.2020.148723.

[21] Krishnapriya, R., S. Praneetha, and A. Murugan. "Investigation of the Effect of Reaction Parameters on the Microwave-Assisted Hydrothermal Synthesis of Hierarchical Jasmine-Flower-Like ZnO Nanostructures for Dye-Sensitized Solar Cells." New Journal of Chemistry 40 (2016): 5080-5089. https://doi.org/10.1039/C6NJ00457A.

[22] Zak, K., W. H. A. Majid, H. Wang, R. Yousefi, M. Golsheikh, and Z. Ren. "Sonochemical Synthesis of Hierarchical ZnO Nanostructures." Ultrasonics Sonochemistry 20, no. 1 (2013): 395-400. https://doi.org/10.1016/j.ultsonch.2012.07.001.

[23] Sarkar, L., M. Sushma, B. Yalagala, A. Rengan, S. Singh, and S. Vanjari. "ZnO Nanoparticles Embedded Silk Fibroin—A Piezoelectric Composite for Nanogenerator Applications." Nanotechnology 33 (2022). https://doi.org/10.1088/1361-6528/ac5d9f.

[24] Qiu, Y., et al. "Controlled Growth of ZnO Nanorods on Common Paper Substrate and Their Application for Flexible Piezoelectric Nanogenerators." Journal of Materials Science: Materials in Electronics 25 (2014): 2649-2656. https://doi.org/10.1007/s10854-014-1924-0.

[25] Mohammad, M. F. M., Muhammad Faizal Abd Halim, Kelvin Alvin Eswar, Rabiatuladawiyah Md Akhir, Najwa Ezira Ahmed Azhar, Nurfazianawatie Mohd Zin, Mohamad Hafiz Mamat, Zuraida Khusaimi, Noor Asnida Asli, Mohd Husairi Fadzilah Suhaimi, and Mohamad Rusop Mahmood. "The Study of Zinc Oxide Nanowires Properties Prepared by Modified Microwave-Assisted Sonochemical Deposition Method at Different Solution Concentrations." International Journal of Chemical and Biochemical Sciences 24, no. 7 (2023).

[26] Malek, M. F. "Synthesisation of Zinc Oxide Nanowires via Hybrid Microwave-Assisted Sonochemical Technique at Various Microwave Power." Journal of Mechanical Engineering (2023). https://doi.org/10.24191/jmeche.v20i3.23913.

[27] Abdulrahman, A., S. Ahmed, N. Ahmed, and M. Almessiere. "Enhancement of ZnO Nanorods Properties Using Modified Chemical Bath Deposition Method: Effect of Precursor Concentration." Crystals (2020). https://doi.org/10.3390/cryst10050386.

[28] Villafuerte, J., et al. "Boosting the Piezoelectric Coefficients of Flexible Dynamic Strain Sensors Made of Chemically-Deposited ZnO Nanowires Using Compensatory Sb Doping." Nano Energy 114 (2023): 108599. https://doi.org/10.1016/j.nanoen.2023.108599.

[29] Ahmad, M., et al. "Effects of Group-I Elements on Output Voltage Generation of ZnO Nanowires Based Nanogenerator; Degradation of Screening Effects by Oxidation of Nanowires." Micromachines 13, no. 9 (2022): 1450. https://doi.org/10.3390/mi13091450.

[30] Ahmad, M., et al. "Effects of As, P and Sb on the Output Voltage Generation of ZnO Nanowires Based Nanogenerator: Mitigation of Screening Effect by Using Surface Modified ZnO Nanowires." Vacuum 202 (2022): 111130. https://doi.org/10.1016/j.vacuum.2022.111130.

[31] Cao, V. A., et al. "Enhanced Output Performance of a Flexible Piezoelectric Nanogenerator Realized by Lithium-Doped Zinc Oxide Nanowires Decorated on MXene." ACS Applied Materials & Interfaces 14, no. 23 (2022): 26824-26832. https://doi.org/10.1021/acsami.2c05857.

[32] Chowdhury, A. R., et al. "Lithium Doped Zinc Oxide Based Flexible Piezoelectric-Triboelectric Hybrid Nanogenerator." Nano Energy 61 (2019): 327-336. https://doi.org/10.1016/j.nanoen.2019.04.085.

[33] Mufti, N., A. Dewi, M. Sanusi, A. Taufiq, A. Hidayat, and Sunaryono. "The Enhanced Performance of Piezoelectric Nanogenerator by Increasing Zinc Precursor Concentration During the Growth of ZnO Nanorods on Stainless Steel Foil." Journal of Physics: Conference Series 1572 (2020). https://doi.org/10.1088/1742-6596/1572/1/012077.

[34] Abubakar, S., et al. "Controlled Growth of Semiconducting ZnO Nanorods for Piezoelectric Energy Harvesting-Based Nanogenerators." Nanomaterials 13 (2023). https://doi.org/10.3390/nano13061025.

[35] Salh, R., and M. Ibrahem. "Efficient Synthesis of ZnO as an Electrode of Piezoelectric Nanogenerators." Science Journal of University of Zakho (2024). https://doi.org/10.25271/sjuoz.2024.12.1.1205.

[36] Okeke, I., et al. "Impact of Particle Size and Surface Defects on Antibacterial and Photocatalytic Activities of Undoped and Mg-Doped ZnO Nanoparticles, Biosynthesized Using One-Step Simple Process." Vacuum 187 (2021): 110110. https://doi.org/10.1016/J.VACUUM.2021.110110.

[37] Trenque, I., S. Mornet, É. Duguet, and M. Gaudon. "New Insights into Crystallite Size and Cell Parameters Correlation for ZnO Nanoparticles Obtained from Polyol-Mediated Synthesis." Inorganic Chemistry 52, no. 21 (2013): 12811-12817. https://doi.org/10.1021/ic402152f.

[38] Kaningini, A. G., et al. "Effect of Optimized Precursor Concentration, Temperature, and Doping on Optical Properties of ZnO Nanoparticles Synthesized via a Green Route Using Bush Tea (Athrixia phylicoides DC.) Leaf Extracts." ACS Omega 7 (2022): 31658-31666. https://doi.org/10.1021/acsomega.2c00530.

[39] Sinha, N., et al. "Y-Doped ZnO Nanosheets: Gigantic Piezoelectric Response for an Ultra-Sensitive Flexible Piezoelectric Nanogenerator." Ceramics International 44 (2018): 8582-8590. https://doi.org/10.1016/J.CERAMINT.2018.02.066.

[40] Wang, D., R. Liu, C. Han, B. Tan, Q. Fu, and Z. Liu. "Investigation of Photoelectrochemical Performance under the Piezoelectric Effect Based on Different Zinc Oxide Morphologies." Inorganics (2022). https://doi.org/10.3390/inorganics11010011.

[41] Mishra, S., et al. "Enhanced Output of ZnO Nanosheet-Based Piezoelectric Nanogenerator with a Novel Device Structure." Engineering Research Express 3 (2021). https://doi.org/10.1088/2631-8695/ac34c3.